Time- and size-resolved bacterial aerosol dynamics in highly polluted air: new clues for haze formation mechanism

Ting Zhang, Xinyue Li, Minfei Wang, Haoxuan Chen and Maosheng Yao*

State Key Joint Laboratory of Environmental Simulation and Pollution Control, College of Environmental Sciences and Engineering, Peking University, Beijing 100871, China

Submitted to

bioRxiv

*** Corresponding Author:**

Maosheng Yao, PhD
Boya Distinguished Professor
State Key Joint Laboratory of Environmental Simulation and Pollution Control,
College of Environmental Sciences and Engineering,
Peking University, Beijing 100871, China
Email: yao@pku.edu.cn
Ph: +86 01062767282

Jan 6, 2019

Beijing, China

Abstract

Aerosol chemistry is often studied without considering microbial involvements. Here, we have applied a high-volume (1 m^3/min) aerosol sampler and the Micro-Orifice Uniform Deposit Impactor (NanoMoudi) along with molecular and microscopic methods to investigate time-and size-resolved bacterial aerosol dynamics in air. Under high particulate matter (PM) polluted episodes, bacterial aerosols were detected to have a viability up to 50-70% in the 0.56-1 µm size range, at which elevated levels of $SO4^{2-}$, NO^{3-} and NH^{4+} were concurrently observed. Engineered or acclimated for both pharmaceuticals and wastewater treatment, bacteria such as *Psychrobacter* spp., *Massilia* spp., *Acinetobacter* lwoffii, *Exiguobacterium* aurantiacum, and *Bacillus* megaterium were shown to have experienced massive abundance shifts in polluted air on early mornings and late afternoons, on which were previously reported to witness rapid new particle formation events. For example, *Acinetobacter* spp. were shown to account for > 96% abundance at a corresponding $PM_{2.5}$ level of 208 µg/m^3. The bacterial aerosol changes corresponded to the observed $PM_{2.5}$ mass peak shift from 3.2-5.6 µm to the high viability size range of 0.56-1µm. Additionally, it is interesting that elevated levels of soluble Na, Ca, Mg, K, Al, Fe and P elements that are required for bacterial growth were observed to co-occur with those significant bacterial aerosol structure shifts in the air. For particular time-resolved $PM_{2.5}$ pollution episodes, *Acinetobacter* and *Massilia* were shown to alternate in dominating the time-resolved aerosol community structures. The results from a HYSPLIT trajectory model simulation suggested that the role by air mass transport in affecting the observed bacterial

aerosol dynamics could be minor. As an evidence, we found that *Acinetobacter, Psychrobacter*, *Exiguobacterium*, and *Bacillus* genera were emitted into the air with a level of > 3000 CFU/m^3 from a pharmaceutical plant. In addition, high level of VOCs up to 15,030 ppbv, mainly Acetone (61%) and Acetaldehyde (11%), were also detected in the air inside the plant. All the data including size-resolved viability and time-resolved bacterial aerosol dynamics together with their growth conditions detected in the air suggested that airborne bacteria in the size range of 0.56- 1μm could have played important roles for haze formation in Beijing. The results about time- and size-resolved bacterial aerosol dynamics from this work provide a fresh understanding of aerosol chemistry especially in highly polluted air. It is hoped that these findings could lend a support in future cost-effective air pollution control practices.

Keywords: Bacterial aerosol dynamics in the air, Particulate matter, Size-and Time-resolved bacterial aerosol, Aerosol chemistry

1. Introduction

Air pollution has become one of serious environmental challenges facing mankind in modern society. Among many others, the core question about air pollution episode is : what is the driving force for accelerating the rapid fine particle growth in typical haze events? Regarding the $PM_{2.5}$ precursor VOC, some studies report that current models underestimate atmospheric VOC emission and also OH radical reactivity(Whalley et al., 2016). Experiments have shown that a direct source of

71 extremely low volatile organic compounds, i.e., a possible new particle formation
72 precursor, was observed from the OH oxidation of acyclic and exocyclic terpenes and
73 isoprene (Jokinen et al., 2015). In another work, it was found that the new particle
74 formation rate, in addition to one-hour lag in time compared to the observation, in the
75 size range of 6-10 nm was significantly underestimated by WRF-Chem and MALTE-BOX
76 models(Huang et al., 2016). These studies collectively imply that there are some
77 uncertainties and unexpected outcomes in measurements of VOCs, new particles and
78 OH reactivity by both aerosol chemistry models and field campaigns.
79
80 Although biological materials such as bacteria are increasingly being investigated
81 during haze episodes, their roles in the $PM_{2.5}$ formation have never been studied or
82 considered. Thus, it is completely unclear if the biological materials have a role in the
83 haze occurrence. In the past, during the haze episodes the levels of fluorescent
84 bioaerosol (described to be viable) particles were shown to be elevated in the size
85 ranges of less than 1 μm(Wei et al., 2016). In addition, endotoxin, an important
86 bacterial membrane component, was also shown to be twice that on clear days(Wei
87 et al., 2016). In other studies, culturable bacterial levels were shown to be higher
88 during the haze periods than those during clear days(Liu et al., 2018;Gao et al.,
89 2016;Gao et al., 2015a;Cao et al., 2014). Among the bacterial genera, *Bacillales,*
90 *Actinomycetales, Pseudomonadales* were detected to dominate the community(Cao
91 et al., 2014;Pöschl et al., 2010). For climate, evidences show that certain bacteria could
92 serve as an ice nucleator or cloud condensation nuclei (Fröhlich-Nowoisky et al.,

2016;Šantl-Temkiv et al., 2015;Pöschl et al., 2010), and they might undergo metabolisms even at lower temperatures(Price and Sowers, 2004). Unfortunately, all these studies did not consider the microbial roles in atmospheric aerosol chemistry or the formation of haze episodes.

Here, this work was conducted to investigate the following questions: 1) if certain bacteria experience a rapid massive increase at particular times in highly polluted air?; 2) If so, in which size and what are the species?; 3) Are there any differences in bacterial dynamics during day and night time for a typical haze episode? ; 4) If bacterial growth conditions are available in highly polluted air? The answers to these questions will be of great value in providing new insights on the long-sought haze formation mechanism.

2. Materials and methods

2.1 Particulate matters (PM) collection

2.1.1 PM sample collection using the NanoMoudi

Size-resolved particulate matter samples were collected using Micro-Orifice Uniform Deposit Impactor (NanoMoudi) (MSP, USA) with 13 stages (stage 1: 10-18 μm; stage 2: 5.6-10 μm;stage 3: 3.2-5.6 μm; stage 4: 1.8-3.2 μm; stage 5: 1.0-1.8 μm; stage 6: 0.56-1.0 μm; stage 7: 0.32-0.56 μm; stage 8: 0.18-0.32 μm; stage 9: 0.1-0.18 μm; stage 10: 0.056-0.01 μm; stage 11: 0.032-0.056 μm; stage 12: 0.018-0.032 μm; and stage 13: 0.01-0.018 μm) near the Environmental Building on Peking University

115 campus(40°00'N, 116°32'E). For each experiment, the NanoMoudi at a sampling flow
116 rate of 28 L/min was placed at 1.5 m above the ground. For the NanoMoudi
117 experiment, six sets of samples were obtained on 47 mm (stage 1 to 10) and 90 mm
118 (stage 11 to 13) aluminum membranes from Sep. 11, 2017 to Sep.14, 2017, during
119 which a high $PM_{2.5}$ pollution episode occurred. The sampling time was categorized into
120 the day-time (Day): from 7:00 AM to 7:00 PM, and the night-time (Night): from 8:00
121 PM to 6:00 AM.
122
123 Before and after sampling, aluminum membranes on each stage of the sampling
124 device were weighed using a microbalance after conditioned at constant temperature
125 (24.5℃) and humid (50%) for at least 48 h in advance. The membrane with samples
126 on each stage of the NanoMoudi was then placed into a 15 mL tube and soaked in 4
127 mL 0.05% tween 20 water, and the sealed tubes were placed at 4℃ in a shaker
128 operated with a rotation speed of 200 rpm continuously for 4 hours. Finally, all the
129 well-mixed sample extracts were kept at -20℃ immediately before any analysis. For
130 the quality controls, all aluminum membranes and the sampler were washed by
131 absolute ethyl alcohol before use. And blank membranes without the air sampling
132 were also brought to the sampling site which was later incorporated into the sample
133 analysis as the negative control.
134
135 ***2.2 Time-resolved bacterial aerosol samples collected using the HighBioTrap sampler***
136 Between February 2018 and May 2018, air samples were collected for a 24-hr time

period for each day in three different pollution episodes (14 -208 μg/m^3) using the HighBioTrap sampler (Beijing dBlue Tech, Inc, Beijing, China) at an air flow rate of 1000 L/min for 20 min for each sample on Peking University campus (40°00'N, 116°32'E). The detailed sampling protocol was described for the HighBioTrap in our previous work(Chen and Yao, 2018). For each $PM_{2.5}$ pollution episode, particulate matter samples were collected in duplicates using the HighBioTrap at an interval of every 2 or 4 hours on an aluminum membrane coated with 600 μL mineral oil at a height of 1.5 m above the ground. Specific sampling times and meteorological conditions are provided in the Table S1 (Supporting Information). Here, two air samples with 20 m^3 air were collected using the high-volume sampler for each specific time period. As a comparison, bacterial aerosol samples were also collected using the HighBioTrap in a pharmaceutical plant to study the bacterial emissions into the air. After each sampling, the mineral-oil-coated membrane was washed by 1.5 mL 0.05% tween 20 water, then the oil-in-water emulsion was centrifuged to remove the mineral oil supernatant at a speed of 7000 rpm using a centrifuge (5804r, Eppendorf, German). After a mixing process, the sample extracts were kept at -20℃ immediately before any analysis. For total bacteria and their community structures, 78 samples and 2 negative control samples (blank membrane samples) were analyzed using qPCR and Illumina platforms (Sangon Biotech, Inc., Shanghai, China) as described in in Supplementary Text. Besides, bacterial species identifications were also performed using VITKE MS and MICROFLEX as described in Supplementary Text. As a comparison, air samples were also collected using the 4-Channel Particulate Matter Sampler as documented in Supplementary Text.

159 Besides, air samples from a pharmaceutical plant were also collected using Silonite™
160 Classical Canisters (Entech Instruments, Simi Valley, CA 93065), and their
161 corresponding volatile organic compounds (VOCs) levels were further analyzed
162 (Wuhan Tianhong Instruments Co., Ltd.) according to a previously published protocol[34].
163
164 **2.3 PM-borne *Endotoxin assay using the LAL assay, bacterial viability using DNA***
165 ***stain method, and reactive oxygen species (ROS) using DL-Dithiothreitol* (*DTT) assay***
166 The samples collected from the NanoMoudi were first centrifuged at 4℃ at 3000
167 rpm in 10 min, and the supernatants were then transferred to the new tubes for the
168 Limulus amebocyte lysate (LAL) assay. A 5-point standard curve from 0.005 to 50.0
169 EU/ml was generated using 10-fold serial dilutions of endotoxin standards (Control
170 Standard Endotoxin, CSE, Associate of Cape Cod, Inc., Eastham, MA, USA) by
171 endotoxin-free water (LAL Reagent Water, Associate of Cape Cod, Inc., Eastham, MA,
172 USA). The LAL agent (Associate of Cape Cod, Inc., Eastham, MA, USA） diluted in the
173 Glucashield Beta Glucan Inhibiting Buffer (Associate of Cape Cod, Inc., Eastham, MA,
174 USA) was used in the assay according to the manufacturer's guidelines. The standards,
175 negative controls and air samples were pre-incubated and analyzed using a microplate
176 reader running SoftMaxPro 5.4.1 software (SpectraMax 340; Molecular Devices,
177 Sunnyvale, CA) with photometric measurements taken at 37°C every 1min for 60 min
178 at 405 nm. The viability of bacteria in the particulate matters was studied using a
179 live/dead viability kit (L7012 BacLight Viability Kit, Invitrogen) as described in
180 Supplementary Text. PM-borne reactive oxygen species (ROS) and metal analysis for

certain air samples collected were conducted using DTT assay and ICP-MS as documented in Supplementary Text.

2.4 Air mass back-trajectory analysis with cluster

Air mass transport for three-days was studied during certain air pollution episodes using HYSPLIT Trajectory Model(NOAA) via Hysplit 4 software. The climate data from GDAS1(ftp://arlftp.arlhq.noaa.gov/pub/archives/gdas1/) were used for simulation.

3. Statistical analysis

The mass distribution mode differences between the hazy day and clean day were analyzed by two-way ANOVA. Other difference analyses were performed using the paired t-test. All tests were performed using the statistical components from the SigmaPlot 12.5 software. Non-metric Multi-Dimensional Scaling (NMDS) based on Bray-Curtis distance was used to compare bacterial community structures among samples. NMDS was performed by *R* software (version 3.2) with the vegan package 2.0-10. A p-value of 0.05 indicates a statistically significant difference in this work.

4. Results and discussion

4.1 *Size-resolved PM mass and composition during different pollution episodes*

Here, we presented our results about PM loading and bacterial aerosol increases in the air from our 24-hr monitoring of four high PM pollution episodes in Beijing during 2017-2018. On Sept 11-14, 2017, in contrast to peak levels in the size range of

3.2 to 5.6 µm on clear days ($PM_{2.5}$=21.42 µg/m^3), significant $PM_{2.5}$ fraction increases from less than 30% to up to 90% of the total mass were detected in the size range of 0.56 to 1 µm during the haze episodes ($PM_{2.5}$=91.33 µg/m^3) as observed in Figure 1 (A), seconded by those appearing in 0.32-0.56 µm size range. For particles of 0.24-0.74 µm, their mass percentages all increased (p-value<0.001; two-way ANOVA), but others did not decrease significantly (p-value=0.198-0.64) as seen in Figure 1 (A) during the haze episodes. The data observed in Figure 1 (A) are generally in line with other studies in which the same particle size range, i.e., 0.56-1 µm, was detected to have the highest mass increases during typical high PM pollution episodes in Beijing (Sun et al., 2015;Yue et al., 2018). This phenomenon was also observed during the haze episodes in other places, such as Taiwan(Tsai et al., 2012) and Singapore(Behera et al., 2015), though different from the firework-caused air pollution scenario(Jing et al., 2014). Similarly, we have also observed that for both size ranges (0.32-0.56 µm and 0.56-1 µm) metals such as Al, Fe, Mg and Zn have all increased during the haze days (B-day and C-night) (Supporting Information Figure S1). For metal Al, Fe and Zn, more emissions were found in the size range of 0.56 - 1 µm during the day than during the night as shown in Figure S1. Particularly, during the haze episodes (B-day and C-night) high Fe levels were detected in 0.32-0.56 µm size range during the night as observed in Figure S1.

For other trace metals as shown in Supporting Information (Figure S3), two size ranges have not experienced major changes. As for metal As, significant elevation was

detected during the daytime, especially in the size range of 0.32 to 0.56 µm during the haze episode. For the C-Day as referred in Figure 1, the metal As (coal combustion indicator) seemed to have shifted from size of 0.32-0.56 µm during the night to the size of 0.56-1 µm during the day. For Ni, even for the clear day (A) higher concentration levels were detected in the size range 0.56-1 µm, and no elevated levels were detected during the haze episodes, suggesting that Ni contribution from fugitive dusts or industrial activities might be insignificant for the haze formation studied in this work. For both size ranges (0.32-0.56 µm) and (0.56-1 µm), metals such as Mn, Cu, Se, Ba and Pb were detected to have higher levels than those during the clear day. As can be seen from the figure, during the nighttime higher element Se levels were detected for the C-day (higher $PM_{2.5}$ levels) in the size range of 0.32 to 0.56 µm, however during the daytime peak Se levels were found in the size range of 0.56-1 µm, suggesting Se-containing particles have possibly shifted from smaller sizes to larger sizes. Se is an indicator for coal combustion, and its elevated levels in the particle peak size suggest the coal combustion was one of the driving factors for the haze formation.

To further study $PM_{2.5}$ formation during polluted days, we analyzed the K, P, and Ca elements from bio-mass burning in the PM samples for different size ranges as shown in Figure 1 (B) and Figure S3. The data in these figures suggest that the elements such as K might have shifted to different size ranges during the dynamic aerosol processes. Here, we have also studied SO_4^{3-}, NO_3^- and NH_4^+ concentration levels in the particles of 0.32-0.56 µm and 0.56-1 µm, and as observed in Figure 1 (C) their

concentration levels were all elevated during the high pollution episodes (e.g., the C-day with higher NO_2 levels as shown in Figure S2 (Supporting Information)) in contrast to low levels (e.g., the A-day). Literature data show that during a typical haze episode of Beijing sulfate production (Figure S2 showing a higher SO_2 level between 13 and 14, Sept , 2017) is a major contributor to $PM_{2.5}$ increase(Wang et al., 2016). Here, we also investigated the toxicity of size-resolved PM samples collected from different time periods (daytime and nighttime) and found as shown in Figure 1 (D) that for the size ranges of 0.24-0.74 μm the average $PM_{2.5}$ toxicity (oxidative potential) was higher during the night than during the day though at a lower confidence level (p-value= 0.190), suggesting possible particle composition change during the day. For example, metals such as Fe and As, contributors to PM oxidative potential, in smaller sizes were observed here to have shifted to larger ones. Overall, the observed particle loadings and related chemical compositions here agree with those reported in the literature.

4.2 Massive changes in time-resolved bacterial aerosol concentration and viability in highly polluted air

Importantly, we have here observed pronounced bacterial aerosol changes in viability for highly polluted days C-night ($PM_{2.5}$=108 μg/m^3) and B-day ($PM_{2.5}$=80 μg/m^3) as shown using viable bacterial percentages in Figure 2 (A) and Supporting Information (Figure S4, S5). Here, we have simultaneously observed the elevated levels of bacterial growth materials such as ions (NO_3^-, NH_4 , etc) as shown in Figure 1 (C) at the same size ranges as discussed above, which co-occurred with increases in bacterial cells and viability as shown in Figure 2 (A). Through fluorescent microscopic analysis of the size-

resolved PM samples collected using the NanoMoudi as shown in Figure S4, S5 (Supporting Information), we have found that the size-resolved bacterial percentages have varied over the time. For example, as shown in Figure 2 (A) during the low $PM_{2.5}$ day (A-day) most of the bacteria were in the larger size ranges (larger than 1 µm) during the nighttime, however during the daytime the peak (about 22%) shifted to the size range of 0.56-1 µm. Likewise, similar findings were observed for the high $PM_{2.5}$ day (B) except the percentage was detected to be up to 35%. In contrast, for the high $PM_{2.5}$ day (C) the peak significantly decreased from 0.56-1 µm to larger sizes from the nighttime to daytime. The C-day witnessed a decrease of $PM_{2.5}$ levels. For both A-Day and C-Day, the total bacteria have decreased from nighttime to daytime, however for the B-day the total bacteria increased from nighttime to daytime. In addition to microscopic analysis, we have also performed qPCR analysis for the size-resolved bacterial aerosol samples as shown in Figure S6 (Supporting Information). Overall, the qPCR data agreed well with the microscopic data (Supporting Information Figure S4). The total bacteria seemed to have decreased from nighttime to daytime, however for a particular size range, e.g., 0.56-1 µm, their percentages have increased from nighttime to daytime. Overall, these data revealed that bacterial levels in the size ranges of 0.56-1 µm have changed from nighttime to daytime, implying a changing bacterial aerosol dynamic under different time and pollution conditions.

Using BackLight DNA stain method, 50-70% of viable bacteria were found in the size range of 0.56-1 µm as observed in Figure 2 (B) and Figure S4, S5 for the A-day and B-day (haze formation day) during the daytime, while less than 20% of viable bacteria

292 for the C-day (haze disappearing day) was noted. In contrast, during the nighttime, the
293 peak for viable bacteria about 30% was found at 0.32-0.56 µm for B-night, close to 60%
294 found at the 0.56-1 µm for C-night and about 10% for the A-night (Supporting
295 Information Figure S5). The size-resolved percentages of viable bacteria for three
296 different days (A- "biomass burning" day, B-"haze formation"day, C-"haze disappearing"
297 day) were observed to have changed substantially (Supporting Information Figure S5).
298 For dead bacteria, as shown in the figure, in the size range of 0.56-1 µm, higher
299 percentage was observed for the C-day, and the lowest for the B-day (the haze
300 formation day) during the nighttime. However, for the daytime, the highest percentage
301 was observed in the size range of 5.6-10 µm for the C-day (haze disappearing day). The
302 percentages for the A- and B-day were found to be similar as seen in the figure. In this
303 work, we have also analyzed the endotoxin (a bacterial derivative) levels during the
304 nighttime and daytime for three different dates (A, B, and C) as shown in Supporting
305 Information Figure S7. As shown in the figure, for the A- and B-day most of the
306 endotoxin was detected in the smaller size ranges of 0.032 -0.18 µm, while during the
307 daytime most of the endotoxin was detected in the larger sizes of > 3.2 µm. In this
308 work, we have also observed that the endotoxin levels for those hazy days (B and C)
309 were found to be higher than the clear day (A) with lower $PM_{2.5}$ levels for 1-18 µm size
310 range (p-value=0.023), although no statistically significant differences were detected
311 between daytime and nighttime. In a previous work, Wei et al. also reported that
312 endotoxin concentration in the PM was elevated up to 12.4 EU/m^3 during a haze
313 episode in Beijing, about twice that during a clear day(Wei et al., 2016). All the data

314 including the microscopic data (size-resolved percentages of viable bacteria, qPCR,
315 viability and endotoxin, total bacteria) together with favorable bacterial growth
316 conditions suggest that bacteria in the size range of 0.56- 1µm could have played a
317 non-neglected role for air pollution episodes.

318

319 To further understand the problem with bacteria in highly polluted air, we have
320 conducted another three different sets of experiments on May 12-13, 2018, March 10-
321 12, 2018, and Feb 6-7, 2018. Different from the first NanoMoudi experiment, we took
322 time-resolved air samples (20 m^3 air for 20 min) using a high-volume sampler
323 (HighBioTrap, dBlueTech Co., Ltd, Beijing China) every two hours for different time
324 periods to capture the bacterial growth events. As seen from Figure 2 (A, B, C), at 16:00
325 of May 12 with a $PM_{2.5}$ level up to 160 µg/m^3, we have detected a significantly higher
326 bacterial aerosol concentration using qPCR, which also corresponded to higher viable
327 bacterial levels (53,037 cells/m^3) as detected using DNA stain (Figure 2 (C)). For other
328 time periods, the bacterial aerosol concentration levels were detected to decrease
329 substantially (2 hours after the high PM episode) as shown in Figure 2 (B) down to
330 1689 cells/m^3 as shown in Figure 2 (A) by qPCR; Figure 2 (B) and Figure 2 (E) by DNA
331 stain, respectively for different $PM_{2.5}$ levels. Figure 2 (F) shows the culturable bacteria
332 for 1.33 m^3 air sampled during different $PM_{2.5}$ levels, and the results were comparable
333 to those detected using DNA stain method as shown in Figure 2 (C), Figure 2 (D) and
334 Figure 2 (E). As observed in Figure 2 (F), substantially higher bacterial concentration
335 levels were observed for higher $PM_{2.5}$ levels (160 µg/m^3). Wei et al. reported that the

336 viable bioaerosol particle concentration increased over a 6-fold at night or early dawn
337 during the haze episode compared with that on clean day(Wei et al., 2016). Culturable
338 bacteria concentrations during the haze days were also observed to be higher than
339 those during the non-haze days(Li et al., 2015). In another work aerosolized bacteria
340 were shown to experience metabolic activity in the simulated air state when supplied
341 with carbon source (Krumins et al., 2014). However, Amato et al. reported that after
342 the 18h aerosolization of the bacteria into the air its cultivable bacterial percentage if
343 without adding nutrients started to decrease down to 4% (Amato et al., 2015). Our
344 data from qPCR, DNA stain, and culturing in these sets of experiments as illustrated in
345 Figure 2 further reveal that massive changes in time-resolved bacterial aerosol
346 dynamics are taking place in highly polluted air, e.g., during haze episodes in Beijing.
347

348 **4.3** ***Massive time-resolved bacterial community structure shifts in highly polluted air***

349 To further investigate the specific bacterial species that have experienced the
350 massive changes in the polluted air, the collected air samples were sequenced and also
351 analyzed using ion chromatography methods (both VITEK MS and Microflex). Here, we
352 have found as shown in Figure 3 (A) that during clear days (14 to 93 μg/m^3) as a control
353 on Feb 6-7, 2018 regardless of the sampling time periods, the bacterial structures
354 remained to be relatively uniform for most of the studied time. Nonetheless, we have
355 still detected a difference in bacterial structures as seen in Figure 3 (A) for the time of
356 20:00PM on Feb 6, 2018, showing an increase in abundances of *Ralstonia* and
357 *Acinetobacter*. Interestingly, this event also co-occurred with a higher $PM_{2.5}$ level, i.e.,

75 μg/m^3. For the clear day, among those bacterial genera detected, *Ralstonia* and *Acinetobacter* were found to be most abundant. Besides, *Psychrobacter* and *Massilia* were also detected among the top 20 genera. In contrast, as shown in Figure 3 (B) the bacterial structures varied greatly within a day during the haze days ($PM_{2.5}$ level up to 251 μg/m^3) on March 10-12, 2018. Among the bacterial genera detected, *Psychrobacter, Massilia*, *Acinetobacter*, and *Arthrobacter* were found to dominate the community structure. During low level of air pollution episodes as shown in Figure 3 (A), *Ralstonia* was detected to be the second dominant species up to 4.16-14.66%, however during high pollution episodes ($PM_{2.5}$ concentration up to 251 μg/m^3), *Ralstonia* was found to only account for 0-0.78% of the total abundances, a substantial decrease. For certain time periods (from 8:00 AM on March 11 to 12:00 AM on March 13), as observed in Figure 3 (B) when the $PM_{2.5}$ levels increased the relative abundances of *Psychrobacter*, *Massilia* and *Acinetobacter* witnessed sharp increases up to about 96% at the corresponding $PM_{2.5}$ level of 208 μg/m^3. The bacterial community structure differences are much visible as seen by the genus heatmap shown in Figure 3 (C) for March 10-12, 2018.

To further investigate the problem and confirm these findings, we have conducted another set of different experiments on May 12, 2018 using similar methods. In contrast to other experiments, culturable *Acinetobacter lwoffii, Bacillus cereus, Bacillus pumilus*, *Exiguobacterium aurantiacum*, *Arthrobacter ilicis*, *Bacillus cereus*, *Bacillus megaterium*, *Coriobacterium* were detected to be abundant using colorimetry

methods including VITKE MS (BioMérieux) and microflex (Bruker) (two methods confirmed with each other for specific species) as seen in Figure 3 (D) and Figure 3 (E). Among these species, *Acinetobacter lwoffii, Exiguobacterium aurantiacum*, and *Bacillus pumilus* were found to be most abundant. *Bacillus pumilus* and *Exiguobacterium aurantiacum* are often used in wastewater treatment practices, while *Acinetobacter lwoffii* is a human pathogen. The differences observed in bacterial aerosol dynamics in different PM pollution episodes indicate that air pollution episodes could varied from one to another in their characteristics. For low and high PM pollution levels, the bacterial aerosol dynamics appeared to be very different. For low level PM pollution, the bacterial aerosol structures remained to be relatively constant, in contrast bacterial structures experienced rapid changes during the day not only in abundances but also in species, e.g., several species such as *Psychrobacter* could account for more than 90% of the total abundance as shown in Figure 3 (B). Among the detected species, *Psychrobacter* is a psychrophilic bacterium and used in wastewater treatment(Huang et al., 2018), while *Massilia* is also used in degrading water-borne PAH(Chadhain et al., 2006). The results obtained in this repeated experiment on a different haze day further strengthen the fact that rapid and time-resolved massive changes in bacterial aerosol dynamics have taken place for different $PM_{2.5}$ pollution levels.

Additionally, it is highly interesting that as shown in Figure 4 (A) for the same time, i.e., at 20:00PM on Feb 6, 2018 elevated levels of soluble Na, Ca,Mg, K, Al, Fe and P

were observed, which co-occurred with significant bacterial aerosol species shift (*Acinetobacter* increased significantly) as observed in Figure 3 (A). The Ca ion level was observed more than 0.55 μg /m^3, followed by Na, Mg, K and others as shown in Figure 4 (A). These element ions are necessary for bacterial growth. Likewise, for March 10-13 experiments, several different ion peaks were observed as shown in Figure 4 (B). For those samples collected at 20:00PM of March 11 ("11-20" in the figure) and 08:00AM of March 12 ("12-8" in the figure), elevated Ca, Na and Mg levels were also observed up to 0.9 μg /m^3 for Ca ion , corresponding to significant bacterial aerosol shifts as observed in Figure 3 (B). It seems that as observed in Figure 3 (B) and Figure 4 (B) *Acinetobacter* and *Massilia* alternated to dominate the bacterial aerosol community structures. When Ca ion level increased *Acinetobacter* started to dominate, while Na level increased *Massilia* started to dominate. The co-occurrence of time-resolved element ion elevation with time-resolved bacterial aerosol structure shift suggest the ions must have been to some extent related to bacterial aerosol dynamics in the air. In addition, we have also constructed a HYSPLIT Trajectory Model for air mass transport for March 10-13, 2018 experiment as shown in Figure 5. As seen from the figure, during the episode air mass was transported from four different directions with different contributions up to 30% of the total transport. In addition, as shown in Figure 5 along the transport directions most of $PM_{2.5}$ levels were below 100 μg/m^3. Accordingly, it is hard to believe that regional air mass transport contributed directly to the rapid shifts in bacterial aerosol structure shifts, viability and levels.

4.4 *A new frame for understanding air pollution episodes*

Air pollution has resulted in tremendous loss of life and economy every year worldwide. Huge amount of research has already been devoted to studying the haze formation and the aerosol chemistry mechanisms(Wang et al., 2006;Zhao et al., 2013;Liu et al., 2013). However, microbial aerosols rarely been considered to play a role in aerosol chemistry especially in highly polluted air. Previously, we have shown using a laser-induced fluorescence-based method that the viable bacterial aerosol concentration was significantly elevated during high $PM_{2.5}$ pollution episodes in Beijing(Wei et al., 2016). Here, for the first time we have captured the size-and time-resolved massive microbial level increase and structure shift events in high $PM_{2.5}$ polluted air in Beijing using a high-volume portable aerosol sampler up to 1000 L/min. Traditionally, people often use low flow rate sampler such as BioSampler (SKC, INc., flow rate=12.5 L/min) and the 4-channel PM sampler (16.7 L/min) or sometimes up to 100 L/min, but most for short time samplings(Gao et al., 2015b;Yuan et al., 2017). These samplers with low sampling rates often fail to capture rapid but transient microbial events in the air since newly bacterial aerosol dynamics could be quickly diluted by open ambient air, and such time-resolved events could also discontinue as atmospheric conditions change from the air. For example, through NMDS analysis we detected a difference in bacterial community structures in the samples collected by the HighBioTrap sampler, but not those collected using the 4-Channel PM sampler (16.7 L/min) as shown in Figure S9 (Supporting Information). Here, by applying a high volume sampler we were able to successfully capture the time-resolved changes in

446 microbial aerosol dynamics in the air.

447

448 Accordingly, based on the results obtained here we hypothesize a new haze
449 formation mechanism, i.e., some new aerosol chemistry for highly polluted air as
450 illustrated in Figure 6. As depicted from the figure, bacteria are presumed to be
451 emitted from ground due to various human activities into the air. As such an evidence
452 shown in Figure S10, we found that the bacterial aerosol concentration level exceeded
453 3000 CFU/m^3 in a pharmaceutical plant in China. In addition, sequence data shown in
454 Figure S11 (Supporting Information) showed that *Acinetobacter*, *Psychrobacter,*
455 *Exiguobacterium*, and *Bacillus* genera were emitted and detected to dominate
456 airborne bacterial community in workshop air inside the pharmaceutical plant. As
457 discussed, these bacteria were also detected in the ambient air in Beijing during the
458 haze episodes, and some of these bacteria experienced rapid concentration changes
459 in the air as presented in Figure 3. Besides, the total VOC concentration for one
460 chimney (pharmaceutical waste treatment workshop) inside the plant was observed
461 to reach a level of 15,030 ppbv, which mainly consisted Acetone (61%) and
462 Acetaldehyde (11%) as seen in Figure S12(Supporting Information). These data support
463 our claim that ground human activities such as pharmacy producing could emit large
464 amounts of bacteria into the air, which were also detected in highly polluted air. As
465 detected in the air samples in this work, the nutrients for bacterial growth such as NH_4^+,
466 NO_3^-, Ca, Na, K, Mg, etc. along with other favorable conditions such as RH and gases
467 are readily available in highly polluted atmosphere such as haze episodes in Beijing,

accordingly providing required conditions for bacterial growth. Accordingly, we hypothesize that the bacterial growth in the air could have taken place during air pollution episodes as depicted in Figure 6. The bacterial growth typically can undergo for different cycles (in general ~20-30 min per cycle), depending on the availability of various conditions such as nutrients, RH and temperature. As hypothesized in Figure 6, for typical high PM pollution episodes, atmospheric boundary layer is lowered(Quan et al., 2014), thus leading to increases in ambient pollutant concentrations such as VOC, NH_3, NOx, etc. Under these conditions, the airborne bacteria such as *Acinetobacter lwoffii*, *Bacillus* cereus, *Bacillus pumilus*, *Exiguobacterium aurantiacum*, *Arthrobacter ilicis*, *Bacillus cereus, Bacillus megaterium*, *Coriobacterium* emitted from ground human activities, e.g., as demonstrated from a pharmaceutical or a wastewater treatment plant, as hypothesized in Figure 6 can play an important role for atmospheric carbon and nitrogen cycles during their growth, thus influencing aerosol chemistry.

Studies show that bacteria can use VOC as nutrient(Paavolainen et al., 1998;Krumins et al., 2014), degrade PAH(Chadhain et al., 2006), oxidize NOx(Lambeth, 2004) and scavenge OH radicals(Samake et al., 2017), and at the same time bacteria can also release many mVOCs during their growth(Schulz and Dickschat, 2007). According to the literature, these mVOCs are often small molecular weight molecules (<300 Da) such as hydrocarbons, alcohols, aldehydes and ketones), terpenoids, aromatic compounds, nitrogen containing compounds and volatile sulphur

compounds(Lemfack et al., 2013). For example, *Acinetobacter calcoaceticus* can emit 2-oxoethanesulfonic Acid (LogP=-1.18; $C_2H_4O_4S$) (Schulz and Dickschat, 2007) which is classified as a sulfate and belongs to semi-volatile VOC (sVOC). And *Pseudomonas fluorescens* can emit low volatility Methylsulfonylsulfanylmethane ($C_2H_6O_2S_2$, LogP= -0.06)(Hunziker et al., 2014). In this work, we also detected higher abundance of *Acinetobacter* during higher PM pollution episodes. On the other hand, *Ralstonia solanacearum* can emit nitrogen containing compounds such as 2-chloro-2-nitropropane ($C_3H_6ClNO_2$)(Spraker et al., 2014). In our work, we have detected higher abundance of *Ralstonia* species in our work as shown in Figure 3 A). In another work, it was shown that *Psychrobacter* spp. can emit 2,3-Dimethyl-oxirane, 2-Butanone, 2-Formylhistamine, 2-Methyl-2-propanol, Acetaldehyde, Acetone, Ethylene oxide, Isopropylalcohol, and Trimethylamine(Broekaert et al., 2013). For a complete reference to mVOC emitted by both bacteria and fungi, there is a database available in the literature(Lemfack et al., 2013). As seen from the database, bacteria, depending on the species type, could emit mVOCs containing sulfur, nitrogen or simply hydrocarbon[35]. These smaller molecules (mVOCs) can be further oxidized into ultrafine particles under oxidizing environments, and some of them are sVOC with lower vapor pressure.

These analyses led to our belief that the bacterial growth, accordingly emitting mVOCs as new particle precursors, in the air could play a very important role for new particle formation as hypothesized in Figure 6. From the literature, we have found that

512 new particle formation occurred during the early mornings (04:00-06:00) or during the
513 afternoon time period (18:00-22:00) (Liu et al., 2008;Wang et al., 2014). During these
514 same time periods, massive changes in bacterial aerosol levels and structure shifts
515 were also observed in our work as shown in Figure 1-3. As illustrated in Figure 6, these
516 ultrafine particles eventually could grow into fine particles via hydroscopic growth or
517 through atmospheric oxidization(Guo et al., 2014). Depending on the bacterial species
518 or the ambient pollutants, major components of the sVOC ultrafine particles emitted
519 if any in the air as hypothesized could be organic compounds, nitrogen containing or
520 sulfates, thus likely impacting haze episode dynamics. Simultaneously, airborne
521 bacteria can also scavenge OH radicals(Samake et al., 2017) and react with metals such
522 as Fe(Chen et al., 2013) in the water layer as depicted in Figure 6. During a certain time
523 period, the available nutrients for bacteria are depleting in the atmosphere, then the
524 bacterial growth may slow down and eventually stop. From our observations, these
525 bacteria are mostly in the size range 0.5-1 μm, and those newly produced ones can be
526 quickly attached by atmospheric ultrafine particles or form aggregates, which could
527 later grow into bigger particles and settle to the ground. When the latter occurs, the
528 high PM pollution episode is disappearing. Here, some psychrophilic bacteria were
529 also detected, indicating microbial growth in the cold air could also occur, e.g., during
530 the winter periods when frequent hazes occur. Those bacteria trained for engineering
531 purposes can also significantly impact human health and ecology when they have
532 undergone growth if any in the air and further precipitated into the local environments
533 or inhaled by humans during high air pollution episodes. For example, we have

534 detected abundant human pathogen such as *Acinetobacter lwoffii* in highly polluted
535 air, which thus presents a significant public health concern. The hypothesized bacterial
536 growth in the air partly could explain the underestimates (e.g. HCHO was
537 underestimated by about 16% compared to observation) of atmospheric VOCs by
538 current models, and also the under-prediction (about 30%) of OH radical loss rate (OH
539 radicals react with VOCs)(Whalley et al., 2016). Here, we only investigated the bacterial
540 dynamics, while those airborne fungal species could also have an impact in the air
541 under favorable conditions. This work was mainly conducted in Beijing, and certainly
542 many other urban settings are warranted to further verify the findings from this work.
543 The results from this work provide a new understanding of current aerosol chemistry
544 known so far especially in highly polluted air. The relevant results might find their
545 values in future cost-effective air pollution control practices. The hypothesized
546 airborne bacterial growth mechanism can be explored using an isotope-based
547 experimental method in future studies.
548

549 **5.Acknowledgements**

550 This study was supported by the NSFC Distinguished Young Scholars Fund Awarded
551 to M. Yao (21725701), and the National Natural Science Foundation of China (Grants
552 91543126, 21611130103, 21477003, 41121004), the Ministry of Science and
553 Technology (grants 2016YFC0207102, 2015CB553401, and 2015DFG92040).
554

555 6.**Author contribution**

556 MY designed the study, TZ performed the experiments, XL, MW helped conducting some of
557 the samplings, XL, HC collected the air samples from the pharmaceutical plant. TZ and MY
558 prepared the manuscript with contributions from all co-authors. The results here only
559 represent scientific evidences and the authors' understanding of the problem.

560

561 **7. References**

562 Amato, P., Joly, M., Schaupp, C., Attard, E., Möhler, O., Morris, C., Brunet, Y., and Delort,
563 A.-M.: Survival and ice nucleation activity of bacteria as aerosols in a cloud simulation
564 chamber, Atmospheric Chemistry and Physics, 15, 6455-6465, doi:10.5194/acp-15-
565 6455-2015, 2015.

566 Behera, S. N., Betha, R., Huang, X., and Balasubramanian, R.: Characterization and
567 estimation of human airway deposition of size-resolved particulate-bound trace
568 elements during a recent haze episode in Southeast Asia, Environmental Science and
569 Pollution Research, 22, 4265-4280, doi:10.1007/s11356-014-3645-6, 2015.

570 Broekaert, K., Noseda, B., Heyndrickx, M., Vlaemynck, G., and Devlieghere, F.: Volatile
571 compounds associated with Psychrobacter spp. and Pseudoalteromonas spp., the
572 dominant microbiota of brown shrimp (Crangon crangon) during aerobic storage,
573 International Journal of Food Microbiology, 166, 487-493,
574 doi:10.1016/j.ijfoodmicro.2013.08.013, 2013.

575 Cao, C., Jiang, W., Wang, B., Fang, J., Lang, J., Tian, G., Jiang, J., and Zhu, T. F.: Inhalable
576 microorganisms in Beijing's PM2. 5 and PM10 pollutants during a severe smog event,
577 Environmental Science & Technology, 48, 1499-1507, doi:10.1021/es4048472, 2014.

578 Chadhain, S. M. N., Norman, R. S., Pesce, K. V., Kukor, J. J., and Zylstra, G. J.: Microbial
579 dioxygenase gene population shifts during polycyclic aromatic hydrocarbon
580 biodegradation, Applied and Environmental Microbiology, 72, 4078-4087, doi:
581 10.1128/AEM.02969-05, 2006.
582 Chen, H., and Yao, M.: A high-flow portable biological aerosol trap (HighBioTrap) for
583 rapid microbial detection, Journal of Aerosol Science, 117, 212-223, doi:
584 10.1016/j.jaerosci.2017.11.012, 2018.
585 Chen, Q., Li, J., Wu, Y., Shen, F., and Yao, M.: Biological responses of Gram-positive and
586 Gram-negative bacteria to nZVI (Fe 0), Fe 2+ and Fe 3+, RSC Advances, 3, 13835-13842,
587 doi: 10.1039/C3RA40570B, 2013.
588 Fröhlich-Nowoisky, J., Kampf, C. J., Weber, B., Huffman, J. A., Pöhlker, C., Andreae, M.
589 O., Lang-Yona, N., Burrows, S. M., Gunthe, S. S., and Elbert, W.: Bioaerosols in the Earth
590 system: Climate, health, and ecosystem interactions, Atmospheric Research, 182, 346-
591 376, doi: 10.1016/j.atmosres.2016.07.018, 2016.
592 Gao, J.-F., Fan, X.-Y., Pan, K.-L., Li, H.-Y., and Sun, L.-X.: Diversity, abundance and activity
593 of ammonia-oxidizing microorganisms in fine particulate matter, Scientific Reports, 6,
594 38785, doi: 10.1038/srep38785, 2016.
595 Gao, M., Jia, R., Qiu, T., Han, M., Song, Y., and Wang, X.: Seasonal size distribution of
596 airborne culturable bacteria and fungi and preliminary estimation of their deposition
597 in human lungs during non-haze and haze days, Atmospheric Environment, 118, 203-
598 210, doi: 10.1016/j.atmosenv.2015.08.004, 2015a.
599 Gao, M., Qiu, T., Jia, R., Han, M., Song, Y., and Wang, X.: Concentration and size

distribution of viable bioaerosols during non-haze and haze days in Beijing, Environmental Science and Pollution Research, 22, 4359-4368, doi: 10.1007/s11356-014-3675-0, 2015b.

Guo, S., Hu, M., Zamora, M. L., Peng, J., Shang, D., Zheng, J., Du, Z., Wu, Z., Shao, M., and Zeng, L.: Elucidating severe urban haze formation in China, Proceedings of the National Academy of Sciences, 111, 17373-17378, doi: 10.1073/pnas.1419604111, 2014.

Huang, X., Ding, A., Liu, L., Liu, Q., Ding, K., Niu, X., Nie, W., Xu, Z., Chi, X., and Wang, M.: Effects of aerosol-radiation interaction on precipitation during biomass-burning season in East China, Atmospheric Chemistry & Physics, 16, 10063–10082, doi:10.5194/acp-16-10063-2016, 2016.

Huang, Z., Wang, Y., Jiang, L., Xu, B., Wang, Y., Zhao, H., and Zhou, W.: Mechanism and performance of a self-flocculating marine bacterium in saline wastewater treatment, Chemical Engineering Journal, 334, 732-740, doi: 10.1016/j.cej.2017.10.076, 2018.

Hunziker, L., Bönisch, D., Groenhagen, U., Bailly, A., Schulz, S., and Weisskopf, L.: Pseudomonas strains naturally associated with potato plants produce volatiles with high inhibition potential against Phytophthora infestans, Applied and Environmental Microbiology, 8,821-830, doi: 10.1128/AEM.02999-14, 2015.

Jing, H., Li, Y.-F., Zhao, J., Li, B., Sun, J., Chen, R., Gao, Y., and Chen, C.: Wide-range particle characterization and elemental concentration in Beijing aerosol during the 2013 Spring Festival, Environmental Pollution, 192, 204-211, doi: 10.1016/j.envpol.2014.06.003, 2014.

622 Jokinen, T., Berndt, T., Makkonen, R., Kerminen, V.-M., Junninen, H., Paasonen, P.,
623 Stratmann, F., Herrmann, H., Guenther, A. B., and Worsnop, D. R.: Production of
624 extremely low volatile organic compounds from biogenic emissions: Measured yields
625 and atmospheric implications, Proceedings of the National Academy of Sciences,
626 11,7123-7128, doi: 10.1073/pnas.1423977112, 2015.
627 Krumins, V., Mainelis, G., Kerkhof, L. J., and Fennell, D. E.: Substrate-dependent rRNA
628 production in an airborne bacterium, Environmental Science & Technology Letters, 1,
629 376-381, doi: 10.1021/ez500245y, 2014.
630 Lambeth, J. D.: NOX enzymes and the biology of reactive oxygen, Nature Reviews
631 Immunology, 4, 181-189, doi: 10.1038/nri1312, 2004.
632 Lemfack, M. C., Nickel, J., Dunkel, M., Preissner, R., and Piechulla, B.: mVOC: a database
633 of microbial volatiles, Nucleic Acids Research, 42, D744-D748, doi:
634 10.1093/nar/gkt1250 2013.
635 Li, Y., Fu, H., Wang, W., Liu, J., Meng, Q., and Wang, W.: Characteristics of bacterial and
636 fungal aerosols during the autumn haze days in Xi'an, China, Atmospheric Environment,
637 122, 439-447, doi: 10.1016/j.atmosenv.2015.09.070, 2015.
638 Liu, H., Zhang, X., Zhang, H., Yao, X., Zhou, M., Wang, J., He, Z., Zhang, H., Lou, L., and
639 Mao, W.: Effect of air pollution on the total bacteria and pathogenic bacteria in
640 different sizes of particulate matter, Environmental Pollution, 233, 483-493, doi:
641 10.1016/j.envpol.2017.10.070, 2018.
642 Liu, S., Hu, M., Wu, Z., Wehner, B., Wiedensohler, A., and Cheng, Y.: Aerosol number
643 size distribution and new particle formation at a rural/coastal site in Pearl River Delta

644 (PRD) of China, Atmospheric Environment, 42, 6275-6283, doi:
645 10.1016/j.atmosenv.2008.01.063, 2008.
646 Liu, X., Li, J., Qu, Y., Han, T., Hou, L., Gu, J., Chen, C., Yang, Y., Liu, X., and Yang, T.:
647 Formation and evolution mechanism of regional haze: a case study in the megacity
648 Beijing, China, Atmospheric Chemistry & Physics, 12, 16259-16292, doi:10.5194/acp-
649 13-4501-2013, 2013.
650 Paavolainen, L., Kitunen, V., and Smolander, A.: Inhibition of nitrification in forest soil
651 by monoterpenes, Plant and Soil, 205, 147-154, doi: 10.1023/A:100433541, 1998.
652 Pöschl, U., Martin, S., Sinha, B., Chen, Q., Gunthe, S., Huffman, J., Borrmann, S., Farmer,
653 D., Garland, R., and Helas, G.: Rainforest aerosols as biogenic nuclei of clouds and
654 precipitation in the Amazon, Science, 329, 1513-1516, doi: 10.1126/science.1191056 ,
655 2010.
656 Price, P. B., and Sowers, T.: Temperature dependence of metabolic rates for microbial
657 growth, maintenance, and survival, Proceedings of the National Academy of Sciences,
658 101, 4631-4636, doi: 10.1073/pnas.0400522101, 2004.
659 Quan, J., Tie, X., Zhang, Q., Liu, Q., Li, X., Gao, Y., and Zhao, D.: Characteristics of heavy
660 aerosol pollution during the 2012–2013 winter in Beijing, China, Atmospheric
661 Environment, 88, 83-89, doi: 10.1016/j.atmosenv.2014.01.058, 2014.
662 Samake, A., Uzu, G., Martins, J., Calas, A., Vince, E., Parat, S., and Jaffrezo, J.: The
663 unexpected role of bioaerosols in the Oxidative Potential of PM, Scientific Reports, 7,
664 10978, doi: 10.1038/s41598-017-11178-0, 2017.
665 Š antl-Temkiv, T., Sahyoun, M., Finster, K., Hartmann, S., Augustin-Bauditz, S.,

Stratmann, F., Wex, H., Clauss, T., Nielsen, N. W., and Sørensen, J. H.: Characterization of airborne ice-nucleation-active bacteria and bacterial fragments, Atmospheric Environment, 109, 105-117, doi: 10.1016/j.atmosenv.2015.02.060, 2015.

Schulz, S., and Dickschat, J. S.: Bacterial volatiles: the smell of small organisms, Natural Product Reports, 24, 814-842, doi: 10.1039/B507392H, 2007.

Spraker, J. E., Jewell, K., Roze, L. V., Scherf, J., Ndagano, D., Beaudry, R., Linz, J. E., Allen, C., and Keller, N. P.: A volatile relationship: profiling an inter-kingdom dialogue between two plant pathogens, *Ralstonia* solanacearum and *Aspergillus* flavus, Journal of Chemical Ecology, 40, 502-513, doi: 10.1007/s10886-014-0432-2, 2014.

Sun, K., Liu, X., Gu, J., Li, Y., Qu, Y., An, J., Wang, J., Zhang, Y., Hu, M., and Zhang, F.: Chemical characterization of size-resolved aerosols in four seasons and hazy days in the megacity Beijing of China, Journal of Environmental Sciences, 32, 155-167, doi: 10.1016/j.jes.2014.12.020, 2015.

Tsai, J.-H., Lin, J.-H., Yao, Y.-C., and Chiang, H.-L.: Size distribution and water soluble ions of ambient particulate matter on episode and non-episode days in Southern Taiwan, Aerosol and Air Quality Research, 12, 263-274, doi: 10.4209/aaqr.2011.10.0167, 2012.

Wang, G., Zhang, R., Gomez, M. E., Yang, L., Zamora, M. L., Hu, M., Lin, Y., Peng, J., Guo, S., and Meng, J.: Persistent sulfate formation from London Fog to Chinese haze, Proceedings of the National Academy of Sciences, 113, 13630-13635, doi: 10.1073/pnas.1616540113, 2016.

Wang, H., Zhu, B., Shen, L., An, J., Yin, Y., and Kang, H.: Number size distribution of

688 aerosols at Mt. Huang and Nanjing in the Yangtze River Delta, China: Effects of air
689 masses and characteristics of new particle formation, Atmospheric Research, 150, 42-
690 56, doi: 10.1016/j.atmosres.2014.07.020, 2014.
691 Wang, Y., Zhuang, G., Sun, Y., and An, Z.: The variation of characteristics and formation
692 mechanisms of aerosols in dust, haze, and clear days in Beijing, Atmospheric
693 Environment, 40, 6579-6591, doi: 10.1016/j.atmosenv.2006.05.066, 2006.
694 Wei, K., Zou, Z., Zheng, Y., Li, J., Shen, F., Wu, C.-y., Wu, Y., Hu, M., and Yao, M.: Ambient
695 bioaerosol particle dynamics observed during haze and sunny days in Beijing, Science
696 of the Total Environment, 550, 751-759, doi: 10.1016/j.scitotenv.2016.01.137, 2016.
697 Whalley, L., Stone, D., Bandy, B., Dunmore, R., Hamilton, J. F., Hopkins, J., Lee, J. D.,
698 Lewis, A. C., and Heard, D. E.: Atmospheric OH reactivity in central London:
699 observations, model predictions and estimates of in situ ozone production,
700 Atmospheric Chemistry and Physics, 16, 2109-2122, doi: 10.5194/acp-16-2109-2016,
701 2016.
702 Yuan, H., Zhang, D., Shi, Y., Li, B., Yang, J., Yu, X., Chen, N., and Kakikawa, M.: Cell
703 concentration, viability and culture composition of airborne bacteria during a dust
704 event in Beijing, Journal of Environmental Sciences, 55, 33-40, doi:
705 10.1016/j.jes.2016.03.033, 2017.
706 Yue, Y., Chen, H., Setyan, A., Elser, M., Dietrich, M., Li, J., Zhang, T., Zhang, X., Zheng, Y.,
707 Wang, J., and Yao, M.: Size-resolved endotoxin and oxidative potential of ambient
708 particles in Beijing and Zürich, Environmental Science & Technology, 52 , 6816–6824,
709 doi: 10.1021/acs.est.8b01167, 2018.

710 Zhao, X., Zhao, P., Xu, J., Meng, W., Pu, W., Dong, F., He, D., and Shi, Q.: Analysis of a
711 winter regional haze event and its formation mechanism in the North China Plain,
712 Atmospheric Chemistry & Physics, 13, 5685-5696, doi: 10.5194/acp-13-5685-2013,
713 2013.

714

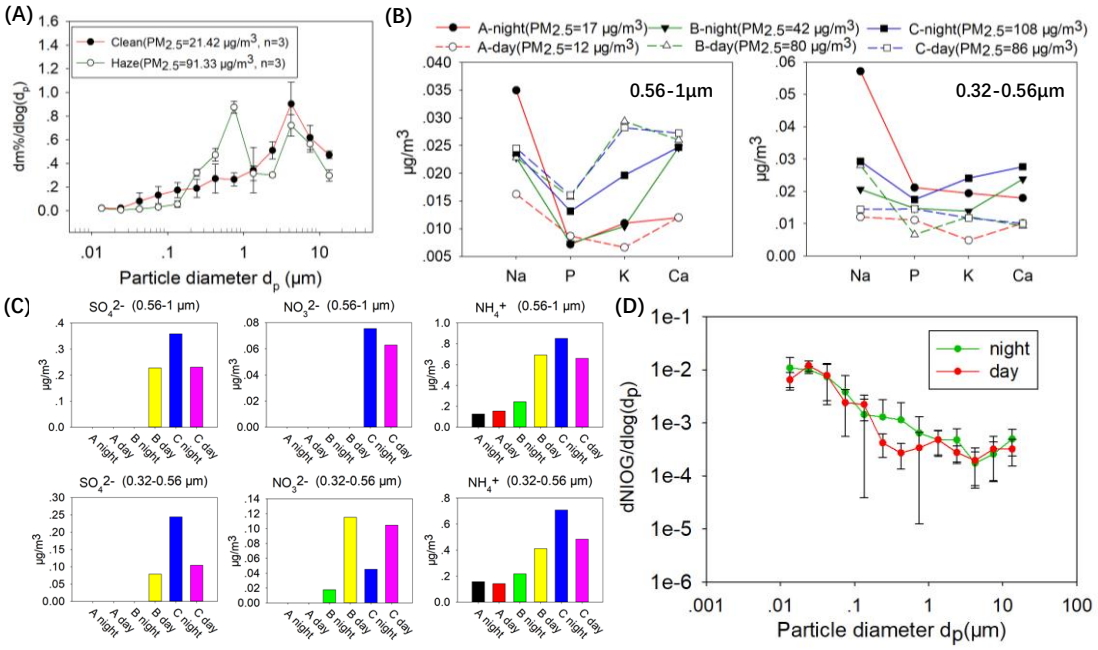

715

716 **Figure 1** Rapid particle increase during typical high PM pollution episodes on Sept 11-
717 14, 2017: A) size-resolved particle mass percentage distribution during low (21.42
718 μg/m^3) and high (91.33 μg/m^3) pollution levels ($PM_{2.5}$ values are averages of three
719 different days (Sept 11-14, 2017); B) Na, P, K, Ca concentration levels in particles of
720 0.56-1 μm and 0.32-0.56 μm during different time periods (Day: 7:00AM-19:00PM;
721 Night: 20:00PM-6:00AM on Sept 11-14, 2017) under different PM pollution levels
722 ($PM_{2.5}$=12-108 μg/m^3); C) SO_4^{2-}, NO_3^- , and NH_4^+ concentration levels measured using
723 Ion Chromatography (Thermo Scientific, Dionex, ICS 2000 and ICS 2500) in particles
724 of 0.56-1 μm and 0.32-0.56 μm under different PM pollution levels on Sept 11-14, 2017;

(Corresponding O_3, NO_2, SO_2, CO concentration levels are shown in Supporting Information Figure S2) ; D) Size-resolved (10 nm-20 μm) particle toxicity measured using DTT method during night and day as shown in Figure 1 (B). Air samples were collected using the NanoMoudi sampler at a flow rate of 28 L/min for 12 hours during the Day (7:00 AM to 19:00PM) and 10 hours during the Night (20:00PM to 6:00AM) on Sept 11-13, 2017.

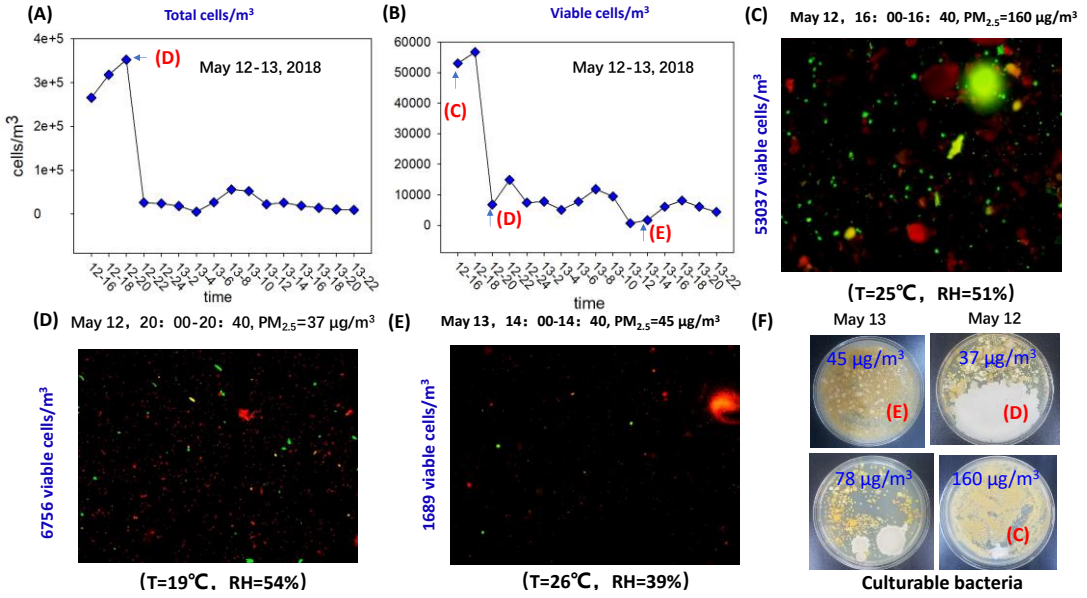

Figure 2 Time-resolved bacterial aerosol dynamics in highly polluted air: A) Total bacterial aerosol concentration levels detected at different times on May 12-13, 2018 using qPCR; B) Total viable bacterial aerosol particle concentration measured using BackLight DNA stain method for different time periods (the digit separated by "-" represent date and time, respectively, e.g., "12-22" means 22:00PM on May 12) during May 12-13, 2018 under different air pollution levels (37 -160 μg/m^3) ($PM_{2.5}$ levels for different time periods of May 12-13 are presented in Supporting Information Figure S8); C) Example image of bacterial DNA stain results from air samples collected

741 during a high $PM_{2.5}$ pollution episode ($PM_{2.5}$=160 μg/m^3 at 20:00-20:40 on May 12,
742 2018); D) Example image of bacterial DNA stain results from air samples collected
743 during a low level $PM_{2.5}$ pollution episode ($PM_{2.5}$=37 μg/m^3 at 16:00-16:40 on May 12,
744 2018); E) Bacterial DNA stain results from air samples collected during a medium level
745 $PM_{2.5}$ pollution episode ($PM_{2.5}$=45 μg/m^3 at 14:00-14:40 on May 13, 2018); F) Example
746 images of bacterial aerosol culturing agar plates (1.33 m^3 air collected using the
747 HighBioTrap) under different $PM_{2.5}$ mass levels during May 12-13, 2018.
748

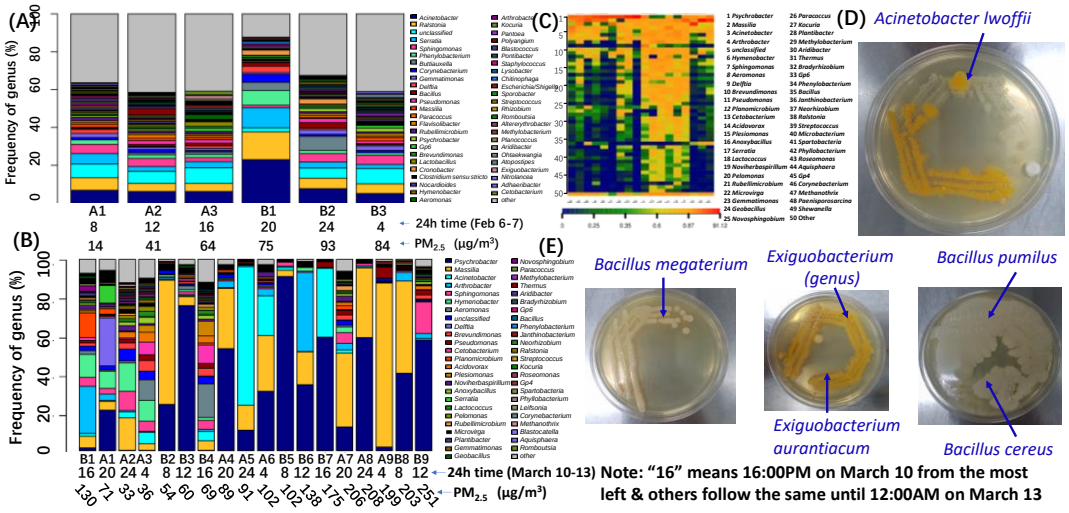

749

750 **Figure 3** Dynamics of bacterial community structures for different time periods during
751 typical pollution processes: (A) Bacterial community structures (on Feb 6- 7, 2018) with
752 $PM_{2.5}$ levels from 14 to 93 μg/m^3; (B) Bacterial community structures (from March 10
753 to 12, 2018) with $PM_{2.5}$ levels from 33 to 251 μg/m^3; (C) Heatmap of bacterial genera
754 structures as shown in Figure 3 (B) on March 10-12, 2018 ; (D) Culturable bacterial
755 isolates detected during May 12, 2018 high $PM_{2.5}$ pollution episodes as shown in Figure
756 2; Two air samples were collected using the HighBioTrap for 20 min each at a flow rate
757 of 1000 L/min, and the samples after the culturing were analyzed using VITKE MS

758 (BioMérieux) and microflex (Bruker) for their corresponding bacterial species;
759 *Acinetobacter lwoffii* and *Exiguobacterium aurantiacum* were found to be most
760 abundant.

761

762

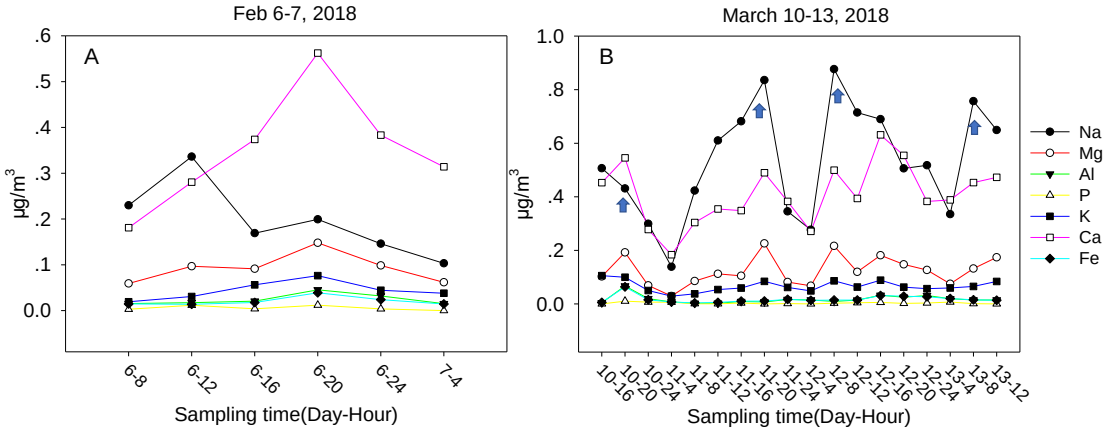

763

764 **Figure 4** Time-resolved soluble elements (Na, Mg, Al, P, K, Ca, and Fe) concentrations
765 in PM samples collected using the HighBioTrap sampler as described in Figure 3 during
766 Feb 6-7, 2018 and March 10-13, 2018 experiments: A) Feb 6-7, 2018; and B) March 10-
767 13,2018.

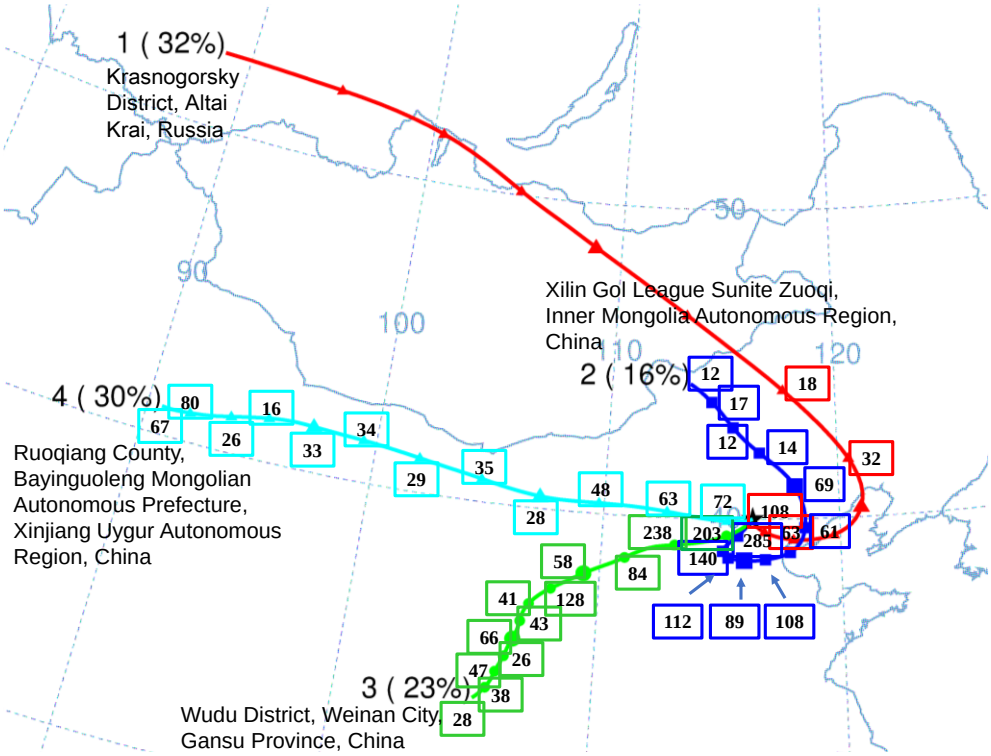

768

769 **Figure 5** Air mass transport to Beijing (39.99 N 116.32 E) during the March 10-13, 2018

770 air pollution episodes using HYSPLIT Trajectory Model (NOAA) via Hysplit 4 software.

771 Numbers on four different lines represent different $PM_{2.5}$ mass concentration levels

772 (http://pm25.in/) ($\mu g/m^3$) when the air mass across. The air mass was transported

773 from 4 different directions (1-4) as marked in the figure, accounting for 32%, 16%, 23%

774 and 30% of the total transport contribution (not estimated for its absolute mass

775 amount).

776

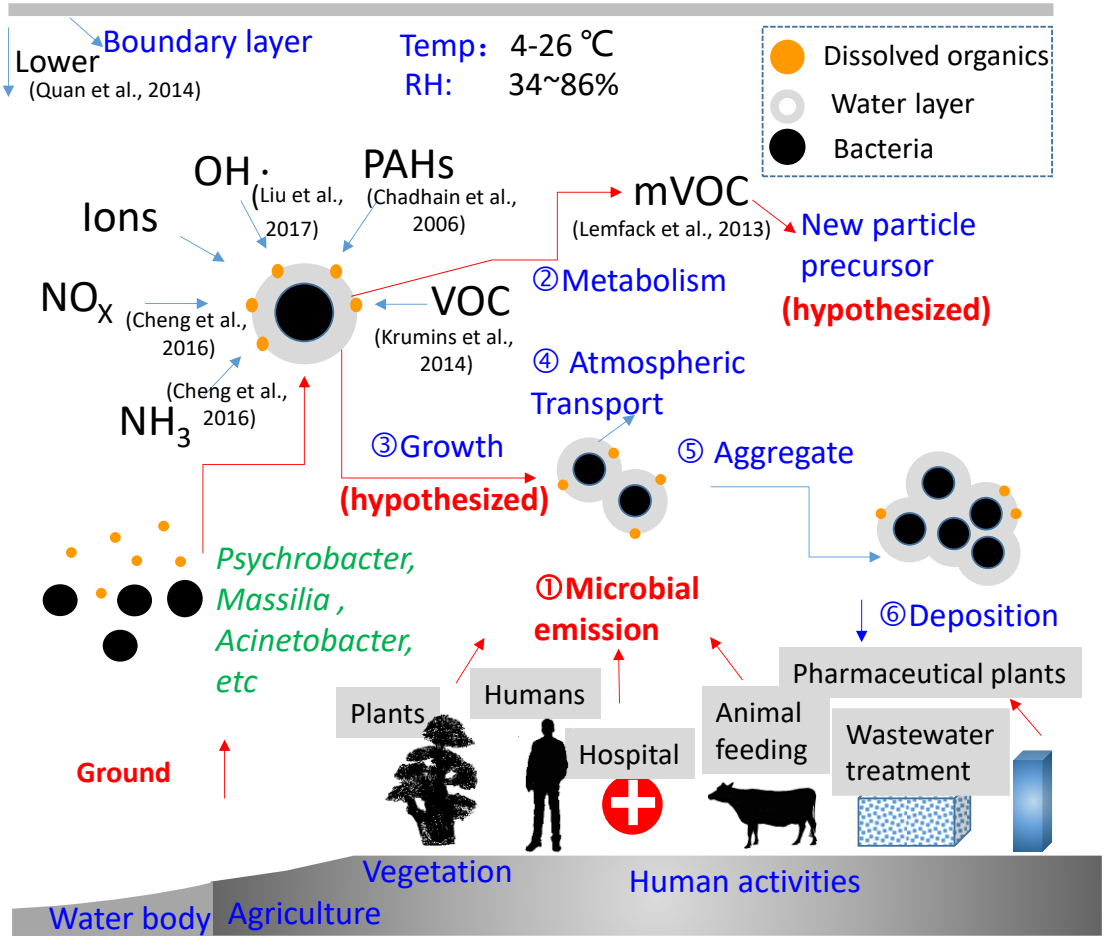

Figure 6 Hypothesized new mechanisms of bacterial growth in the air and possible roles in aerosol chemistry: Ground-emitted bacteria can uptake water vapor, PAH, VOC, NH_3, NOx and release mVOCs during the growth; mVOCs could serve as new particle precursors; ultrafine particles (dissolved organics) can attach to the bacterial surface and further mix with water; newly produced bacteria can form aggregates and precipitate.